

An empirical spectroscopic model for eleven electronic states of VO

Qianwei Qu, Sergei N. Yurchenko and Jonathan Tennyson¹

^aDepartment of Physics and Astronomy, University College London, London, WC1E 6BT, United Kingdom

Abstract

Previously-determined empirical energy levels are used to construct a rovibronic model for the $X^4\Sigma^-$, $A'^4\Phi$, $A^4\Pi$, $B^4\Pi$, $C^4\Sigma^-$, $D^4\Delta$, $1^2\Delta$, $1^2\Sigma^+$, $1^2\Phi$, $1^2\Pi$ and $2^2\Pi$ electronic states of vanadium monoxide. The spectrum of VO is characterized by many couplings and crossings between the states associated with these curves. The model is based on the use of potential energy curves, represented as extended Morse oscillators, and couplings (spin-orbit, spin-spin, angular momentum), represented by polynomials, which are tuned to the data plus an empirical allowance for spin-rotation couplings. The curves are used as input for the variational nuclear motion code Duo. For the $X^4\Sigma^-$, $1^2\Phi$ and $1^2\Pi$ states the model reproduces the observed energy to significantly better than 0.1 cm^{-1} . For the other states the standard deviations are between 0.25 and 1.5 cm^{-1} . Further experimental data and consideration of hyperfine effects would probably be needed to significantly improve this situation.

Keywords: Variational calculations, potential energy curves, spin-orbit coupling

PACS: 0000, 1111

2000 MSC: 0000, 1111

The manuscript has been accepted by the *Journal of Molecular Spectroscopy*

1. Introduction

Vanadium monoxide (VO) is a diatomic molecule with a complicated open shell structure [1, 2]; it absorbs strongly at red and near infrared wavelengths. VO is thought to provide an important source of opacity in the atmospheres of both cool stars [3] and of exoplanets [4, 5]. While VO bands are well-known in the spectrum of cool stars [6] and sunspots [7], only tentative detections have been made in the atmospheres of exoplanets [8, 9, 10, 11, 12, 13, 14]. The charged species VO^- and VO^+ are also important targets of theoretical and experimental studies, see *e.g.*, Miliordos and Mavridis [15] and the references therein.

Theoretically modelling of VO spectra is a challenge both from the perspective of electronic structure calculations [16, 15, 17, 18] and, as will be seen below, from the perspective of representing the nuclear motion due to many resonances between different states. McKemmish *et al.* [19] constructed the so-called VOMYT line list for VO as part of the ExoMol project [20, 21]. The VOMYT line list probably provides a reasonable basis for modelling VO opacities but has been demonstrated to be inadequate for high resolution studies of exoplanetary spectra [22].

The spectrum of VO has been well-studied experimentally [23, 24, 25, 26, 27, 28, 29, 30, 31, 32, 33, 34, 35], see the summary by Bowesman *et al.* [36]; however, the complexity of its spectrum means that there are still important gaps in these studies. Although, as discussed below, our general approach to constructing a spectroscopic model for open shell molecules such as VO is based on variational solutions of the nuclear motion Schrodinger equation, our work on VO [2, 36] and other

open shell molecules [37, 38, 39, 40] has made extensive use of Western's effective Hamiltonian program PGOPHER [41]. We favour the method based on variational solutions as it usually shows much more stable extrapolation properties which is an important feature when one wishes to compute line lists for hot molecules.

In this paper, we attempt to build a spectroscopic model which covers the most important low-lying states of VO, including 6 quartet and 5 doublet electronic states; given the difficulty in fully characterizing the couplings between these state we limit ourselves to considering only the coupling terms necessary to provide a reasonable spectroscopic model. The 11 electronic states considered are shown in Fig. 1; these state are all part of the VOMYT model. They are responsible for the main absorption bands in the near infrared and visible, or are states which are known to interact with them.

The purpose of this work is to provide the basis for a more reliable model than VOMYT as well providing for the quantum number assignments for unassigned recent observations [35, 36]. Thus, our focus is on the accuracy of energy levels and we develop an empirical model that excludes most of the off-diagonal couplings considered in VOMYT [19]. In the recent study by Bowesman *et al.* [36], a spectroscopic network of VO transitions was constructed as a prelude to a MARVEL (measured active rotation vibration energy levels) [42] study of the 11 states involved in this network. The next two sections will demonstrate our effort to reproduce the rovibronic energy levels obtained from the MARVEL study. The other two states ($a^2\Sigma^-$ and $b^2\Gamma$) included in VOMYT [19] were not analyzed in the work of Bowesman *et al.* [36] and are, therefore, excluded from our model as well.

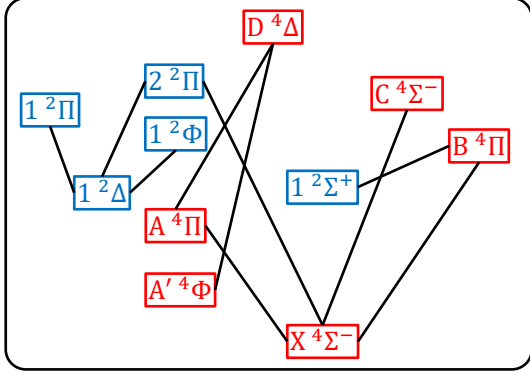


Figure 1: Band systems connecting the 11 electronics included in the model of this work. See Bowesman *et al.* [36] for a more comprehensive diagram.

2. Spectroscopic model

The model was developed using the open-source program for variational calculation of diatomic spectra, Duo¹ [43]. All nuclear motion calculations used 10 vibrationally contracted basis functions for each electronic states based on 401 sinc-DVR grid points, covering the internuclear distance range from 1.2 to 4 Å. The upper bound of the energy was set to 50 000 cm⁻¹, however energy levels of interest for this work are expected to be below 21 000 cm⁻¹. The number of vibrational levels considered for each electronic state is listed in Table 1.

Table 1: Vibrational states considered for each electronic state. Table 5 of Bowesman *et al.* [36] lists the corresponding experimental studies.

Number	States	v
1	X ⁴ Σ ⁻	0-2
2	A' ⁴ Φ	0-2
3	A ⁴ Π	0
4	B ⁴ Π	0-1
5	C ⁴ Σ ⁻	0-2
6	D ⁴ Δ	0-1
9	1 ² Δ	0-1
10	1 ² Σ ⁺	2-3
11	1 ² Φ	0
12	1 ² Π	0-3
13	2 ² Π	0-1

2.1. Potential energy curves

The potential energy curves (PECs) of all states are represented by second-order extended Morse oscillator (EMO) function [44]

$$V(R) = T_e + (D_e - T_e) [1 - \exp(-\beta_{\text{EMO}}(R)(R - R_e))]^2, \quad (1)$$

where R is the internuclear distance, R_e is the equilibrium bond length and T_e is the potential minimum; β_{EMO} is given by the formula:

$$\beta_{\text{EMO}}(R) = b_0 + b_1 y_p(R) + b_2 y_p^2(R), \quad (2)$$

where $y_p(R)$ is:

$$y_p(R) = \frac{R^p - (R_e)^p}{R^p + (R_e)^p}. \quad (3)$$

Duo's users can set independent integer values of p on the left- and right-hand sides of R_e and we chose $p = 4$ for both sides. The parameters of fitted EMO functions are listed in Table 2.

2.2. Diagonal couplings within a electronic state

All coupling curves are represented by low-order polynomials

$$p(R) = a_0 + \sum_{n=1}^{\dots} a_n (R - R_e)^n. \quad (4)$$

Our aim is to use the fewest terms to satisfactorily reproduce the experimental energy levels. Thus, we started with uncoupled PECs for each state and then, added those couplings curves necessary to reduce the fitting errors.

We assume the spin splittings of X⁴Σ⁻ and C⁴Σ⁻ mainly depend on spin-spin coupling terms. Although the assumption is not supported by *ab initio* calculations, *e.g.* see our previous discussion of the X⁴Σ⁻ state[2], this empirical representation can usually give accurate energy levels. Apart from the spin-spin interaction, spin-rotation terms were used to resolve J -dependent spin splittings of ²Σ and ⁴Σ states, where J is the total angular momentum.

In contrast, spin-orbit terms dominate the spin splittings of Π, Δ, Φ and Γ states and are J -dependent too. Therefore, we replaced spin-rotation curves with spin-orbit coupling ones for those states. Spin-spin coupling curves were still used for the quartet states, *i.e.* A'⁴Φ, A⁴Π, B⁴Π and D⁴Δ.

The optimized parameters of diagonal spin-spin, spin-rotation and spin-orbit couplings are listed in Tables 3, 4 and 5, respectively.

We also modeled the Λ -doubling of Π states by using the empirical terms defined by Brown and Merer [45]:

$$\langle \mp 1, \Sigma \pm 2, J, \Omega | \hat{H}_{\text{LD}} | \pm 1, \Sigma, J, \Omega \rangle = \frac{1}{2} (o_v + p_v + q_v) \times \sqrt{[S(S+1) - \Sigma(\Sigma \pm 1)][S(S+1) - (\Sigma \pm 1)(\Sigma \pm 2)]}, \quad (5)$$

$$\langle \mp 1, \Sigma \pm 1, J, \Omega \mp 1 | \hat{H}_{\text{LD}} | \pm 1, \Sigma, J, \Omega \rangle = -\frac{1}{2} (p_v + 2q_v) \times \sqrt{[S(S+1) - \Sigma(\Sigma \pm 1)][J(J+1) - \Omega(\Omega \mp 1)]}, \quad (6)$$

$$\langle \mp 1, \Sigma, J, \Omega \mp 2 | \hat{H}_{\text{LD}} | \pm 1, \Sigma, J, \Omega \rangle = \frac{1}{2} q_v \times \sqrt{[J(J+1) - \Omega(\Omega \mp 1)][J(J+1) - (\Omega \mp 1)(\Omega \mp 2)]}. \quad (7)$$

In these equations, o , p and q depend on vibrational quantum number, v , as Brown and Merer derived the equations based on effective Hamiltonians. In our variational model, we use coupling curves instead. For quartet states, we include all the three coupling curves, while for doublet states, Eq. (5) is automatically zero and we only need the curves of $p + 2q$ and q . The fitted parameters for the $o + p + q$, $p + 2q$ and q curves are listed in Table 6.

¹<https://github.com/exomol/Duo>

Table 2: Optimized extended Morse oscillator (EMO) parameters for the potential energy curves, see Eq.(1).

Number	State	T_e [cm ⁻¹]	R_e [Å]	b_0 [Å ⁻¹]	b_1 [Å ⁻¹]	b_2 [Å ⁻¹]
1	X ⁴ Σ ⁻	0	1.58947260	1.87183393	$6.042\,606\,63 \times 10^{-3}$	$-1.158\,731\,02 \times 10^{-1}$
2	A' ⁴ Φ	7292.4851	1.62591915	1.88461684	$-1.332\,091\,48 \times 10^{-2}$	$1.585\,203\,16 \times 10^{-1}$
3	A ⁴ Π	9534.8342	1.63405670	1.92275217		
4	B ⁴ Π	12659.4107	1.64032109	1.93810207	0	$-2.273\,213\,32 \times 10^{-1}$
5	C ⁴ Σ ⁻	17494.4977	1.67098029	1.94981612	$-5.170\,578\,88 \times 10^{-2}$	$3.271\,206\,99 \times 10^{-1}$
6	D ⁴ Δ	19238.8720	1.68337218	1.91485252	0	3.03001473
7	1 ² Δ	9867.6920	1.58225344	2.06276090	0	$-4.155\,158\,02 \times 10^{-1}$
8	1 ² Σ ⁺	10376.3396	1.57856000	2.15102878	0	$-3.663\,042\,53 \times 10^{-1}$
9	1 ² Φ	15442.9452	1.62904530	2.09925561		
10	1 ² Π	17099.9353	1.62955854	2.10656122	$2.732\,894\,47 \times 10^{-1}$	$1.641\,222\,98 \times 10^{-1}$
11	2 ² Π	18139.4421	1.62244306	2.15748234		

Table 3: Optimized polynomial parameters for diagonal spin-spin coupling curves.

State	a_0 [cm ⁻¹]	a_1 [cm ⁻¹ Å ⁻¹]	a_2 [cm ⁻¹ Å ⁻²]
X ⁴ Σ ⁻	2.05042406	2.76918955	
A' ⁴ Φ	-1.08746355		
A ⁴ Π	1.89104909		
B ⁴ Π	2.62698261		
C ⁴ Σ ⁻	0.73293575		
D ⁴ Δ	1.29783687	0	$-6.220\,435\,54 \times 10^2$

Table 4: Optimized polynomial parameters for diagonal spin-rotation coupling curves.

State	a_0 [cm ⁻¹]	a_1 [cm ⁻¹ Å ⁻¹]
X ⁴ Σ ⁻	$2.143\,878\,41 \times 10^{-2}$	$1.587\,127\,88 \times 10^{-1}$
C ⁴ Σ ⁻	$-1.834\,643\,08 \times 10^{-2}$	
1 ² Σ ⁺	$-7.900\,000\,00 \times 10^{-3}$	

2.2.1. Off-diagonal spin-orbit couplings

We can observe obvious avoided-crossing structures from the rovibronic energy distributions of B⁴Π–1²Σ⁺ and C⁴Σ⁻–2²Π coupled states. Thus, off-diagonal spin-orbit coupling curves, whose parameters are given in Table 7, were introduced to model those structures in crossing regions. The B⁴Π–1²Σ⁺ spin-orbit coupling term was optimized using Duo, while the C⁴Σ⁻–2²Π coupling was manually given an estimated value. See the next section where the results are discussed.

3. Results

3.1. Uncoupled states

The fitting residues of the uncoupled quartet states are given in Fig. 2. The energy levels of X⁴Σ⁻ and A⁴Π are accurately reproduced. Compared with the X⁴Σ⁻ and A⁴Π states, the spin-splittings of A'⁴Φ and D⁴Δ are not well estimated which may arise from electronic state interactions not included in our model. However, the assignment will not be affected as the energy gaps due to spin-orbit couplings of A'⁴Φ and D⁴Δ are usually more than a hundred wavenumbers.

The fitting residues of the uncoupled doublet states are shown in Fig. 3. The doublet states only have two fine structure series

which makes it easier to get good refinement results. The errors for the high- J levels of 1²Δ increase dramatically which is also due to state interactions.

3.2. Coupled states

In our model, B⁴Π–1²Σ⁺ and C⁴Σ⁻–2²Π are coupled by spin-orbit terms to give reasonable avoided crossing structures, as shown from Fig. 4 to Fig. 7.

Figures 4 and 5 demonstrate the smooth transitions from one electronic state to another in both e and f series. Note that, the electronic state quantum numbers of the energy levels near the interaction region are not well-determined. They are assigned according to the dominant contribution of the corresponding basis function to the rovibronic wavefunction. The MARVEL energy levels indicated by the black arrows in these figures were excluded from the fits. They seem to belong to another electronic state but were not recognized in the current model.

The off-diagonal C⁴Σ⁻–2²Π spin-orbit coupling term was not fitted but visually estimated to give an acceptable avoided-crossing structure as shown in Figs. 6 and 7. The $\nu = 0, F_2$ levels of 2²Π shown in Fig. 6 are recently assigned in the work of Bowsman *et al.* [36]. However, the crossing point of this series with F_2 series of C⁴Σ⁻ is different from the previously determined one, as indicated by the black arrow in Fig. 6. All transitions connecting the C⁴Σ⁻ and 2²Π states in the MARVEL spectroscopic network are under review and some of them may be reassigned. Thus, we did not make too much effort to improve the accuracy here.

The $\nu = 0$ levels of C⁴Σ⁻ do not interact with the 2²Π state. Thus, the diagonal spin-rotation coupling term in Table 4 was determined by the states with the $\nu = 0$ levels. Nevertheless,

Table 5: Optimized polynomial parameters for diagonal spin-orbit coupling curves.

State	a_0 [cm ⁻¹]	a_1 [cm ⁻¹ Å ⁻¹]	a_2 [cm ⁻¹ Å ⁻²]	a_3 [cm ⁻¹ Å ⁻³]
A' ⁴ Φ	$2.607\,527\,43 \times 10^2$	$-3.083\,775\,40 \times 10^2$	$-3.019\,871\,04 \times 10^3$	$5.206\,561\,86 \times 10^4$
A ⁴ Π	$5.264\,954\,55 \times 10^1$			
B ⁴ Π	$9.703\,432\,61 \times 10^1$	$-3.312\,045\,51 \times 10^1$		
D ⁴ Δ	$1.390\,545\,88 \times 10^2$	0	$2.599\,205\,12 \times 10^3$	
1 ² Δ	$1.800\,558\,32 \times 10^2$	$-1.587\,723\,00 \times 10^2$		
1 ² Φ	$1.860\,528\,51 \times 10^2$			
1 ² Π	$1.245\,874\,33 \times 10^2$	$8.268\,778\,79 \times 10^1$	$-2.704\,796\,01 \times 10^2$	
2 ² Π	$6.037\,144\,58 \times 10^1$			

Table 6: Optimized polynomial parameters for the $o+p+q$, $p+2q$ and q curves due to Λ -doubling coupling.

Coupling	State	a_0 [cm ⁻¹]
$o+p+q$	A ⁴ Π	2.05253781
	B ⁴ Π	1.20113529
$p+2q$	A ⁴ Π	$-1.416\,923\,02 \times 10^{-2}$
	B ⁴ Π	$3.189\,748\,36 \times 10^{-2}$
	1 ² Π	$-3.121\,071\,39 \times 10^{-2}$
	2 ² Π	$-2.196\,020\,31 \times 10^{-2}$
q	A ⁴ Π	$-2.092\,792\,99 \times 10^{-4}$
	B ⁴ Π	$-1.633\,370\,99 \times 10^{-4}$
	1 ² Π	$-2.043\,450\,34 \times 10^{-4}$
	2 ² Π	$1.002\,402\,89 \times 10^{-3}$

Table 7: Polynomial parameters for the off-diagonal spin-orbit coupling curves.

State	a_0 [cm ⁻¹]
B ⁴ Π - 1 ² Σ ⁺	21.5107379
C ⁴ Σ ⁻ - 2 ² Π	10

there are still systematic errors as shown in Fig. 8. The J -dependent fitting residues of high- J levels should be attributed to C ⁴Σ⁻ - 1 ²Π interaction, although more experimental data are needed to verify this.

3.3. Fitting quality

The root-mean-square error (RMSE) of the fitting residues for each electronic state is calculated as

$$\text{RMSE} = \sqrt{\frac{1}{N} \sum_{i=1}^N e_i^2}, \quad (8)$$

where e_i is the fitting error of the i -th energy level and N is the number of rovibronic states included. The values of RMSE are listed in Table 8.

The VOMYT model was refined using Model Hamiltonian, combination difference energy levels and transition frequencies [19]. As most of the transitions connect to the ground electronic state, VOMYT has a reasonable representation of X ⁴Σ⁻. However, its vibrational structure was still not accurately determined as shown in Fig. 9. There is an obvious offset of the $\nu = 2$ energy levels, which is likely to be significantly worse for higher vibrationally excited states. The RMSE value for the VOMYT model is 0.3015 cm^{-1} , about four times worse than ours.

Table 8: RMSE and maximum absolute error of each state in cm⁻¹.

State	ν	RMSE	Max absolute error
X ⁴ Σ ⁻	0	0.0777	0.2404
	1	0.0168	0.2369
	2	0.0651	0.1884
A' ⁴ Φ	0	0.2241	0.5760
	1	1.3634	2.8620
	2	0.206	0.5821
A ⁴ Π	0	0.1766	0.5131
	1	0.1893	0.9044
D ⁴ Δ	0	0.1893	0.9044
	1	2.3556	4.2883
1 ² Δ	0	0.2675	1.4664
	1	0.2107	0.7573
1 ² Φ	0	0.0507	0.1362
	1	0.0363	0.1380
1 ² Π	0	0.0363	0.1380
	1	0.1145	0.3368
	2	0.0696	0.1217
B ⁴ Π - 1 ² Σ ⁺	2	0.0603	0.1372
	3	0.0603	0.1372
C ⁴ Σ ⁻ - 2 ² Π	0	0.4234	1.2228
	0	0.2949	1.9393
C ⁴ Σ ⁻ - 2 ² Π	0	1.4829	9.0335
	0	1.4829	9.0335

The rotational constants of all states in our model are around 0.5 cm^{-1} and the rotational energy gaps are estimated as

$$\Delta E = 0.5(J+2)(J+1) - 0.5(J+1)J = J+1 \text{ cm}^{-1}. \quad (9)$$

Thus, our model achieves sufficient accuracy to make rotational assignments. The coupling curves can be further refined once revised or extended data is available.

4. Conclusions

We propose an empirical spectroscopic model for 6 quartet and 5 doublet states of VO. The most recent MARVEL analysis of VO [36] generates accurate energy term values for this molecule, which makes it possible to achieve experimental accuracy for some vibronic levels compared with VOMYT [19]. The interactions of B ⁴Π - 1 ²Σ⁺ and C ⁴Σ⁻ - 1 ²Π are analyzed by introducing the off-diagonal spin-orbit couplings between them.

While our model represents a significant advance on what is currently available, there remains two outstanding issues. The

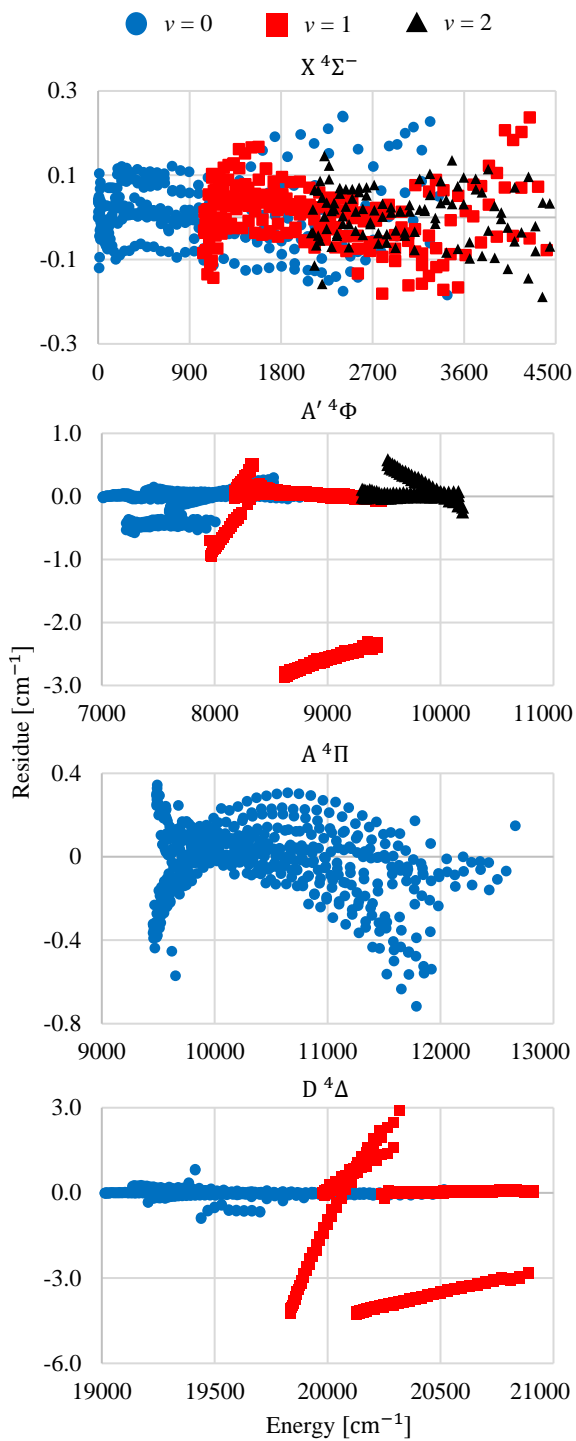


Figure 2: Fitting residues of four uncoupled quartet states: $X^4\Sigma^-$, $A'^4\Phi$, $A^4\Pi$ and $D^4\Delta$.

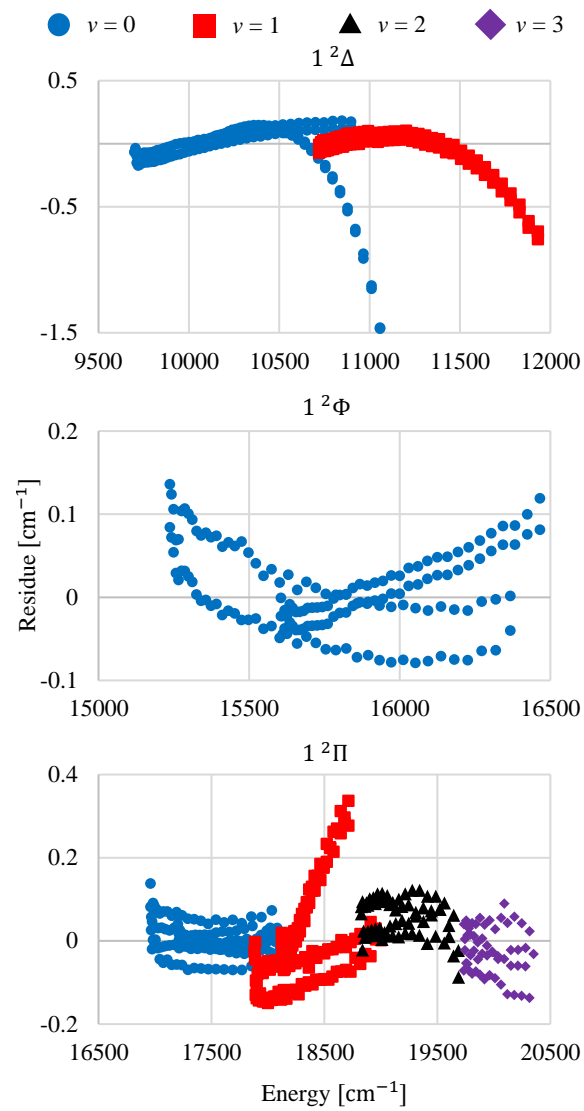


Figure 3: Fitting residues of three uncoupled doublet states: $1^2\Delta$, $1^2\Phi$ and $1^2\Pi$.

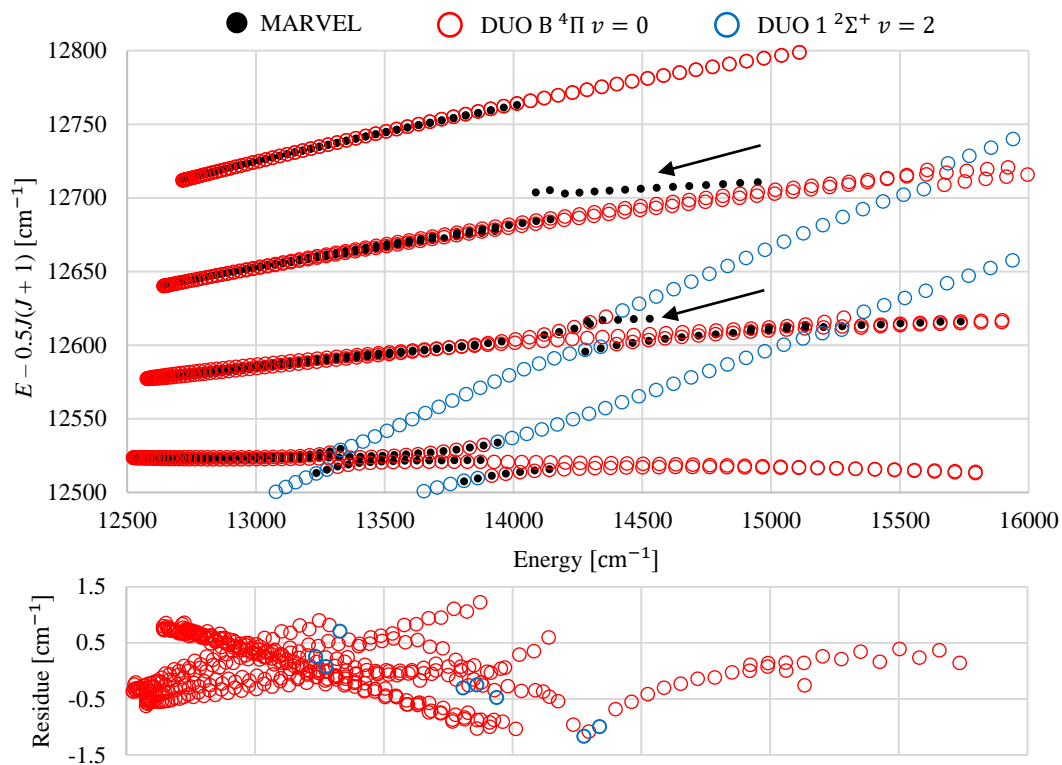


Figure 4: State interaction of $B^4\Pi, \nu = 0$ and $1^2\Sigma^+, \nu = 2$. The black dots in the top panel are the rovibronic energy levels obtained from MARVEL analysis [36] while the circles are the fitting results of Duo. The black arrows indicate some unreasonable data which were excluded in our fitting. The bottom panel shows the fitting residues.

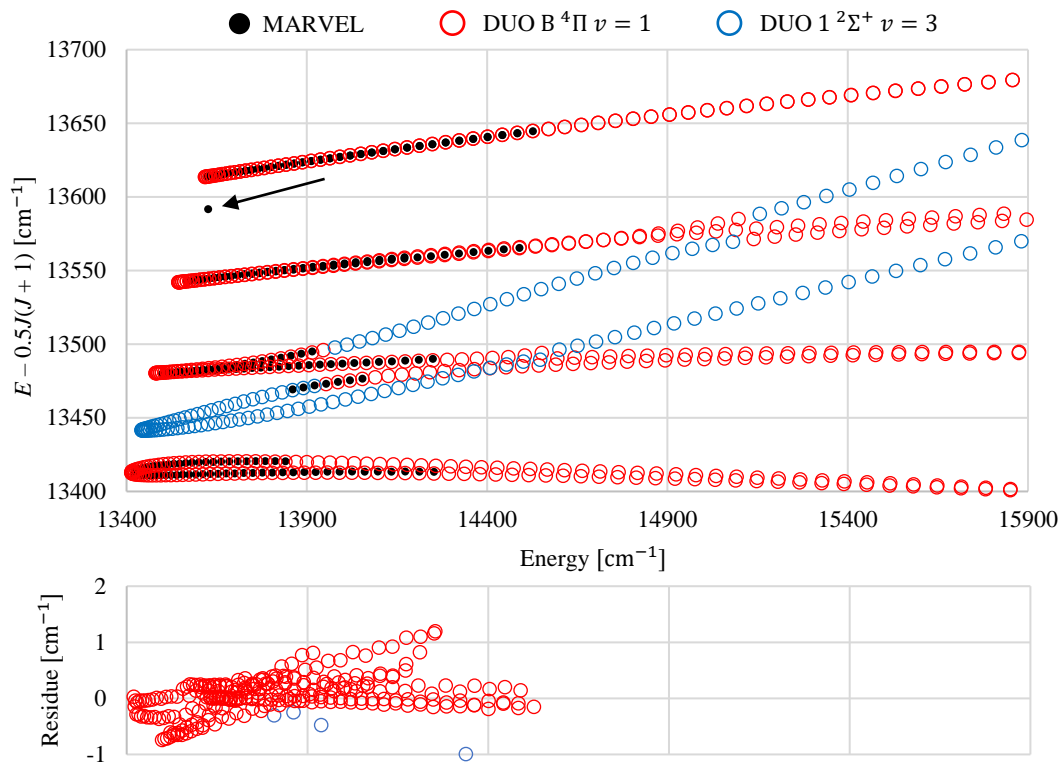


Figure 5: State interaction of $B^4\Pi, \nu = 1$ and $1^2\Sigma^+, \nu = 3$. The black dots in the top panel are the rovibronic energy levels obtained from MARVEL analysis [36] while the circles are the fitting results of Duo. The bottom panel shows the fitting residues.

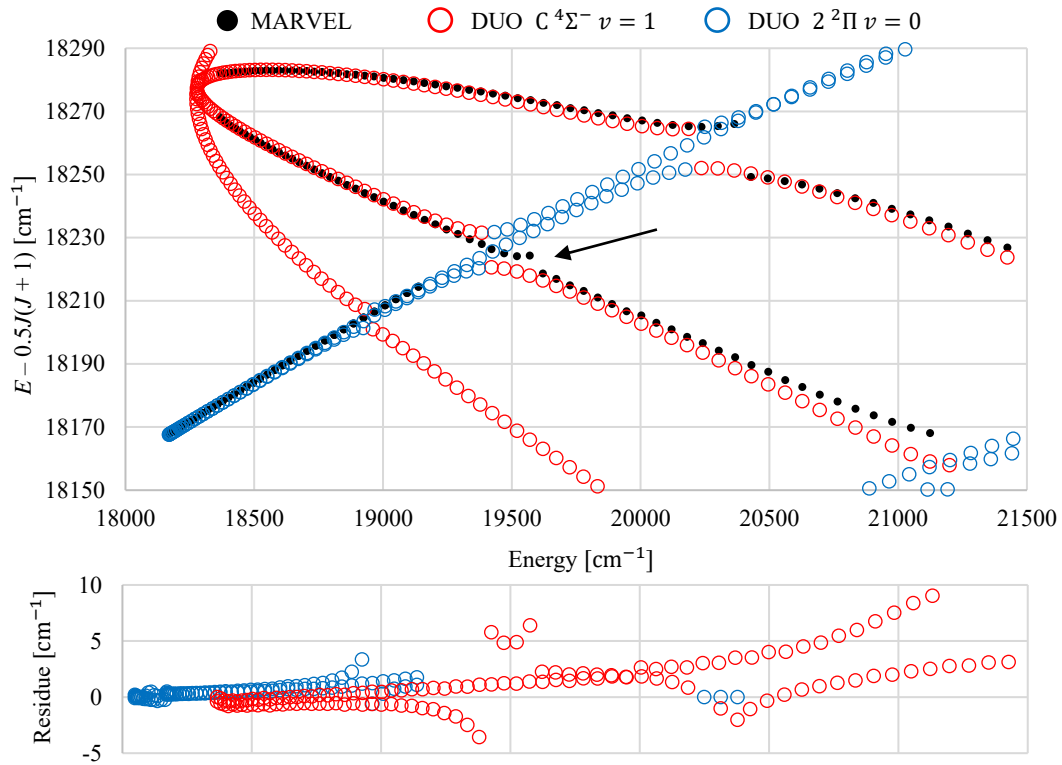


Figure 6: State interaction of $C^4\Sigma^-, \nu = 1$ and $2^2\Pi, \nu = 0$. The black dots in the top panel are the rovibronic energy levels obtained from MARVEL analysis [36] while the circles are the fitting results of Duo. The rotational constant of $2^2\Pi, \nu = 0$ in derived from our model is consistent with that of the recently assigned results (see the blue circles in the top panel). However, its crossing point with the F_2 series of $C^4\Sigma^-, \nu = 1$ is inconsistent with experimental values (see the area pointed by the black arrow). The bottom panel shows the fitting residues.

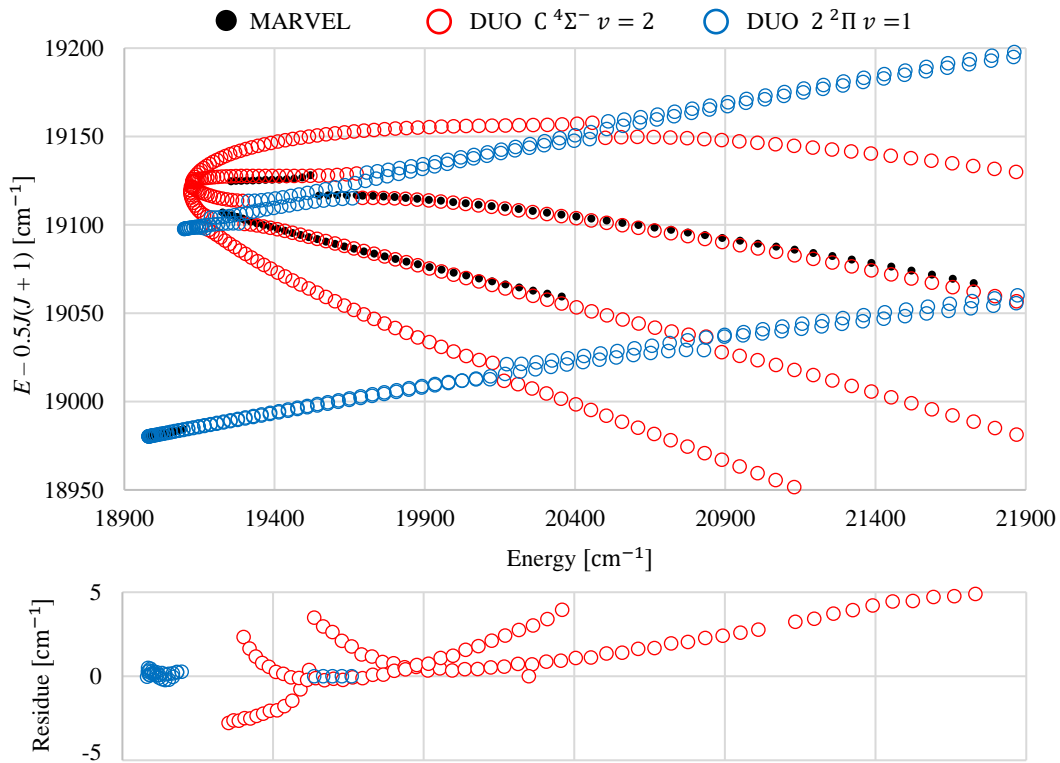


Figure 7: State interaction of $C^4\Sigma^-, \nu = 2$ and $2^2\Pi, \nu = 1$. The black dots in the top panel are the rovibronic energy levels obtained from MARVEL analysis [36] while the circles are the fitting results of Duo. The bottom panel shows the fitting residues.

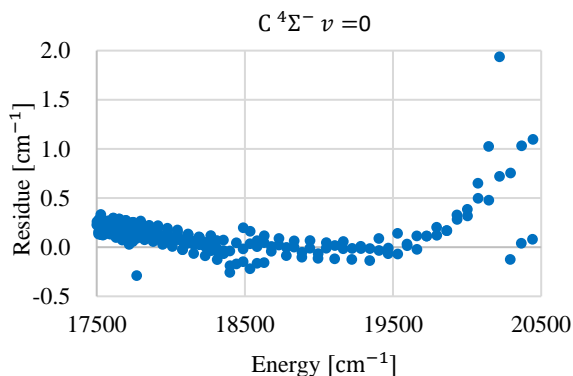


Figure 8: Fitting residues of $C^4\Sigma^-, v=0$.

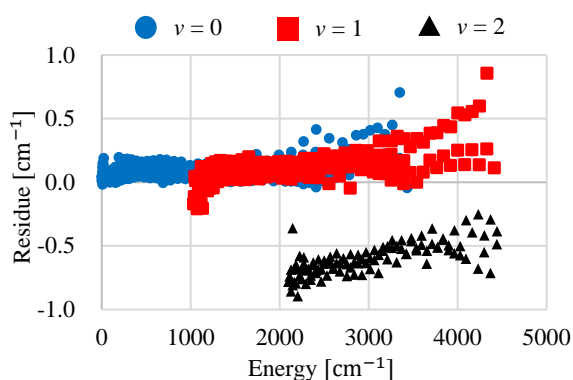


Figure 9: Energy errors for the $X^4\Sigma^-$ state as given by the VOMYT model.

first is the treatment of resonance interactions which is discussed extensively above. Given that state-of-the-art *ab initio* calculations on systems with a transition metal atom are not capable of even approaching the accuracy required for high resolution studies, improving our model will require further experimental input.

The second issue is the hyperfine structure. The main isotope of vanadium, ^{51}V , has a nuclear spin $I = 7/2$ which is known to lead to pronounced hyperfine effects in the spectrum of VO [25, 30, 34]. We have started to address this issue by extending our nuclear motion program Duo to explicitly include hyperfine effects [46] within its variational model. We have also built a hyperfine-resolved spectroscopic model for the ground $X^4\Sigma^-$ state of $^{51}\text{V}^{16}\text{O}$ [2]. We are working on extending the model to other electronic states of VO to give a spectroscopically-accurate, hyperfine-resolved model of the molecule. Given the limited experimental hyperfine-resolved data available for VO, particularly for spectra involving excited vibrational states, further experimental input into this problem would be particularly welcome.

Acknowledgements

We dedicate this article to the memory of Colin Western and acknowledge both the help his work gave to our studies and the readiness with which he responded to our many questions.

Qianwei Qu acknowledges the financial support from University College London and China Scholarship Council. This work was supported by the STFC Projects No. ST/M001334/1 and ST/R000476/1, and ERC Advanced Investigator Project 883830.

Data Availability

The open access programs ExoCross and Duo are available from github.com/exomol. The Duo input file used in this work is given as supplementary material; our potential energy and coupling curves are included as part of this input file.

References

- [1] A. J. Merer, Spectroscopy of the diatomic 3d transition-metal oxides, *Ann. Rev. Phys. Chem.* 40 (1989) 407–438. doi:10.1146/annurev.pc.40.100189.002203.
- [2] Q. Qu, S. N. Yurchenko, J. Tennyson, A variational model for the hyperfine resolved spectrum of VO in its ground electronic state, *J. Chem. Phys.* (2022). doi:10.1063/5.0105965.
- [3] P. F. Bernath, Molecular astronomy of cool stars and sub-stellar objects, *Int. Rev. Phys. Chem.* 28 (2009) 681–709. doi:10.1080/01442350903292442.
- [4] J. J. Fortney, K. Lodders, M. S. Marley, R. S. Freedman, A Unified Theory for the Atmospheres of the Hot and Very Hot Jupiters: Two Classes of Irradiated Atmospheres, *Astrophys. J.* 678 (2008) 1419–1435. doi:10.1086/528370.
- [5] N. Madhusudhan, S. Seager, On the inference of thermal inversions in hot Jupiter atmospheres, *Astrophys. J.* 725 (2010) 261. doi:10.1088/0004-637X/725/1/261.
- [6] R. Tylenda, T. Kamiński, M. Schmidt, R. Kurtev, T. Tomov, High-resolution optical spectroscopy of V838 Monocerotis in 2009, *Astron. Astrophys.* 532 (2011) A138. doi:10.1051/0004-6361/201116858.
- [7] P. Sriramachandran, S. P. Bagare, N. Rajamanickam, K. Balachandrakumar, Presence of LaO, ScO and VO Molecular Lines in Sunspot Umbral Spectra, *Sol. Phys.* 252 (2008) 267–281. doi:10.1007/s11207-008-9261-1.
- [8] T. M. Evans, D. K. Sing, H. R. Wakeford, N. Nikolov, G. E. Ballester, B. Drummond, T. Kataria, N. P. Gibson, D. S. Amundsen, J. Spake, Detection of H_2O and evidence for tio/vo in an ultra-hot exoplanet atmosphere, *Astrophys. J.* 822 (2016) L4. doi:10.3847/2041-8205/822/1/14.
- [9] J. D. Turner, R. M. Leiter, L. I. Biddle, K. A. Pearson, K. K. Hardegree-Ullman, R. M. Thompson, J. K. Teske, I. T. Cates, K. L. Cook, M. P. Berube, M. N. Nieberding, C. K. Jones, B. Raphael, S. Wallace, Z. T. Watson, R. E. Johnson, Investigating the physical properties of transiting hot Jupiters with the 1.5-m Kuiper Telescope, *Mon. Not. R. Astron. Soc.* 472 (2017) 3871–3886. doi:10.1093/mnras/stx2221.
- [10] E. Palle, G. Chen, J. Prieto-Arranz, G. Nowak, F. Murgas, L. Nortmann, D. Pollacco, K. Lam, P. Montanes-Rodriguez, H. Parviainen, N. Casasayas-Barris, Feature-rich transmission spectrum for WASP-127b Cloud-free skies for the puffiest known super-Neptune?, *Astron. Astrophys.* 602 (2017). doi:10.1051/0004-6361/201731018.
- [11] A. Tsiaras, I. P. Waldmann, T. Zingales, M. Rocchetto, G. Morello, M. Damiano, K. Karpouzas, G. Tinetti, L. K. McKemmish, J. Tennyson, S. N. Yurchenko, A population study of gaseous exoplanets, *Astron. J.* 155 (2018) 156. doi:10.3847/1538-3881/aaaf75.
- [12] J. M. Goyal, N. Mayne, B. Drummond, D. K. Sing, E. Hebrard, N. Lewis, P. Tremblin, M. W. Phillips, T. Mikal-Evans, H. R. Wakeford, A library of self-consistent simulated exoplanet atmospheres, *Mon. Not. R. Astron. Soc.* 498 (2020) 4680–4704. doi:10.1093/mnras/staa2300.
- [13] N. K. Lewis, H. R. Wakeford, R. J. MacDonald, J. M. Goyal, D. K. Sing, J. Barstow, D. Powell, T. Kataria, I. Mishra, M. S. Marley, N. E. Batalha, J. I. Moses, P. Gao, T. J. Wilson, K. L. Chubb, T. Mikal-Evans, N. Nikolov, N. Pirzkal, J. J. Spake, K. B. Stevenson, J. Valenti,

- X. Zhang, Into the UV: The Atmosphere of the Hot Jupiter HAT-P-41b Revealed, *Astrophys. J. Lett.* 902 (2020) L19. doi:10.3847/2041-8213/abb77f.
- [14] Q. Changeat, B. Edwards, The hubble WFC3 emission spectrum of the extremely hot jupiter KELT-9b, *Astrophys. J. Lett.* 907 (2021) L22. doi:10.3847/2041-8213/abd84f.
- [15] E. Miliordos, A. Mavridis, Electronic structure of vanadium oxide. Neutral and charged species, $\text{VO}^{0,\pm}$, *J. Phys. Chem. A* 111 (2007) 1953–1965. doi:10.1021/jp067451b.
- [16] T. Rivlin, L. K. McKemmish, K. E. Spinlove, J. Tennyson, Low-temperature scattering with the R-matrix method: from nuclear scattering to atom-atom scattering and beyond, *SciPost Phys. Proc.* (2020).
- [17] L. K. McKemmish, S. N. Yurchenko, J. Tennyson, Ab initio calculations to support accurate modelling of the rovibronic spectroscopy calculations of vanadium monoxide (VO), *Mol. Phys.* 114 (2016) 3232–3248. doi:10.1080/00268976.2016.1225994.
- [18] T. Jiang, Y. Chen, N. A. Bogdanov, E. Wang, A. Alavi, J. Chen, A full configuration interaction quantum Monte Carlo study of ScO, TiO, and VO molecules, *J. Chem. Phys.* (2021) 164302doi:10.1063/5.0046464.
- [19] L. K. McKemmish, S. N. Yurchenko, J. Tennyson, ExoMol Molecular line lists – XVIII. The spectrum of Vanadium Oxide, *Mon. Not. R. Astron. Soc.* 463 (2016) 771–793. doi:10.1093/mnras/stw1969.
- [20] J. Tennyson, S. N. Yurchenko, ExoMol: molecular line lists for exoplanet and other atmospheres, *Mon. Not. R. Astron. Soc.* 425 (2012) 21–33. doi:10.1111/j.1365-2966.2012.21440.x.
- [21] J. Tennyson, S. N. Yurchenko, A. F. Al-Refaie, V. H. J. Clark, K. L. Chubb, E. K. Conway, A. Dewan, M. N. Gorman, C. Hill, A. E. Lynas-Gray, T. Mellor, L. K. McKemmish, A. Owens, O. L. Polyansky, M. Semenov, W. Somogyi, G. Tinetti, A. Upadhyay, I. Waldmann, Y. Wang, S. Wright, O. P. Yurchenko, The 2020 release of the ExoMol database: molecular line lists for exoplanet and other hot atmospheres, *J. Quant. Spectrosc. Radiat. Transf.* 255 (2020) 107228. doi:10.1016/j.jqsrt.2020.107228.
- [22] S. de Regt, A. Y. Kesseli, I. A. G. Snellen, S. R. Merritt, K. L. Chubb, A quantitative assessment of the VO line list: Inaccuracies hamper high-resolution VO detections in exoplanet atmospheres, *Astron. Astrophys.* 661 (2022) A109. doi:10.1051/0004-6361/202142683.
- [23] A. Lagerqvist, L. E. Selin, Rotationsanalyse der sichtbaren Vanadiumoxydbanden, *Arkiv for Fysik* 12 (1957) 553–568.
- [24] W. H. Hocking, A. J. Merer, D. J. Milton, Resolved hyperfine structure in the C–X electronic transition of VO. An internal hyperfine perturbation in the $C^4\Sigma^-$ state, *Can. J. Phys.* 59 (1981) 266–270. doi:10.1139/p81-035.
- [25] A. S.-C. Cheung, R. C. Hansen, A. J. Merer, Laser spectroscopy of VO: Analysis of the rotational and hyperfine structure of the $C^4\Sigma^- - X^4\Sigma^-$ (0, 0) band, *J. Mol. Spectrosc.* 91 (1982) 165–208. doi:10.1016/0022-2852(82)90039-X.
- [26] A. S.-C. Cheung, A. W. Taylor, A. J. Merer, Fourier transform spectroscopy of VO: Rotational structure in the $A^4\Pi - X^4\Sigma^-$ system near 10 500 Å, *J. Mol. Spectrosc.* 92 (1982) 391–409. doi:10.1016/0022-2852(82)90110-2.
- [27] A. J. Merer, G. Huang, A. S.-C. Cheung, A. W. Taylor, New quartet and doublet electronic transitions in the near-infrared emission spectrum of VO, *J. Mol. Spectrosc.* 125 (1987) 465–503. doi:10.1016/0022-2852(87)90110-X.
- [28] R. D. Suenram, G. T. Fraser, F. J. Lovas, C. W. Gillies, Microwave spectra and electric dipole moments of $X^4\Sigma_{12}^-$ VO and NbO, *J. Mol. Spectrosc.* 148 (1991) 114–122. doi:10.1016/0022-2852(91)90040-H.
- [29] A. S.-C. Cheung, P. G. Hajigeorgiou, G. Huang, S. Z. Huang, A. J. Merer, Rotational Structure and Perturbations in the $B^4\Pi - X^4\Sigma^-$ (1, 0) Band of VO, *J. Mol. Spectrosc.* 163 (1994) 443–458. doi:10.1006/jmsp.1994.1039.
- [30] A. G. Adam, M. Barnes, B. Berno, R. D. Bower, A. J. Merer, Rotational and Hyperfine Structure in the $B^4\Pi - X^4\Sigma^-$ (0,0) Band of VO at 7900 Å: Perturbations by the $a^2\Sigma^+$, $v = 2$ Level, *J. Mol. Spectrosc.* 170 (1995) 94–130. doi:10.1006/jmsp.1995.1059.
- [31] L. Karlsson, B. Lindgren, C. Lundevall, U. Sassenberg, Lifetime Measurements of the $A^4\Pi$, $B^4\Pi$, and $C^4\Sigma^-$ States of VO, *J. Mol. Spectrosc.* 181 (1997) 274–278. doi:10.1006/jmsp.1996.7173.
- [32] R. S. Ram, P. F. Bernath, S. P. Davis, A. J. Merer, Fourier Transform Emission Spectroscopy of a New $^2\Phi - 1^2\Delta$ System of VO, *J. Mol. Spectrosc.* 211 (2002) 279–283. doi:10.1006/jmsp.2001.8510.
- [33] R. S. Ram, P. F. Bernath, Emission spectroscopy of a new $^2\Delta - 1^2\Delta$ system of VO, *J. Mol. Spectrosc.* 229 (2005) 57–62. doi:10.1016/j.jms.2004.08.014.
- [34] M. A. Flory, L. M. Ziurys, Submillimeter-wave spectroscopy of VN ($X^3\Delta_r$) and VO ($X^4\Sigma^-$): A study of the hyperfine interactions, *J. Mol. Spectrosc.* 247 (2008) 76–84. doi:10.1016/j.jms.2007.09.007.
- [35] W. S. Hopkins, S. M. Hamilton, S. R. Mackenzie, The electronic spectrum of vanadium monoxide across the visible: New bands and new insight, *J. Chem. Phys.* 130 (2009) 144308. doi:10.1063/1.3104844.
- [36] C. A. Bowersman, H. Akbari, S. Hopkins, S. N. Yurchenko, J. Tennyson, Fine and hyperfine resolved empirical energy levels for VO, *J. Quant. Spectrosc. Radiat. Transf.* 289 (2022) 108295. doi:10.1016/j.jqsrt.2022.108295.
- [37] L. K. McKemmish, T. Masseron, J. Hoeijmakers, V. V. Pérez-Mesa, S. L. Grimm, S. N. Yurchenko, J. Tennyson, ExoMol Molecular line lists – XXXIII. The spectrum of Titanium Oxide, *Mon. Not. R. Astron. Soc.* 488 (2019) 2836–2854. doi:10.1093/mnras/stz1818.
- [38] C. A. Bowersman, M. Shuai, S. N. Yurchenko, J. Tennyson, A high resolution line list for AlO, *Mon. Not. R. Astron. Soc.* 508 (2021) 3181–3193. doi:10.1093/mnras/stab2525.
- [39] S. N. Yurchenko, J. Tennyson, A.-M. Syme, A. Y. Adam, V. H. J. Clark, B. Cooper, C. P. Dobney, S. T. E. Donnelly, M. N. Gorman, A. E. Lynas-Gray, T. Meltzer, A. Owens, Q. Qu, M. Semenov, W. Somogyi, A. Upadhyay, S. Wright, J. C. Zapata Trujillo, ExoMol line lists – XLIV. IR and UV line list for silicon monoxide ($^{28}\text{Si}^{16}\text{O}$), *Mon. Not. R. Astron. Soc.* 510 (2022) 903–919. doi:10.1093/mnras/stab3267.
- [40] M. Semenov, J. Tennyson, S. N. Yurchenko, ExoMol line lists – XLVI: Empirical rovibronic spectra of silicon mononitrate (SiN) covering 6 lowest electronic states and 4 isotopologues, *Phys. Chem. Chem. Phys.* 516 (2022) 1158–1169. doi:10.1093/mnras/stac2004.
- [41] C. M. Western, PGOPHER: A program for simulating rotational, vibrational and electronic spectra, *J. Quant. Spectrosc. Radiat. Transf.* 186 (2017) 221–242. doi:10.1016/j.jqsrt.2016.04.010.
- [42] T. Furtenbacher, A. G. Császár, J. Tennyson, MARVEL: measured active rotational-vibrational energy levels, *J. Mol. Spectrosc.* 245 (2007) 115–125. doi:10.1016/j.jms.2007.07.005.
- [43] S. N. Yurchenko, L. Lodi, J. Tennyson, A. V. Stolyarov, Duo: a general program for calculating spectra of diatomic molecules, *Comput. Phys. Commun.* 202 (2016) 262–275. doi:10.1016/j.cpc.2015.12.021.
- [44] E. G. Lee, J. Y. Seto, T. Hirao, P. F. Bernath, R. J. Le Roy, FTIR emission spectra, molecular constants, and potential curve of ground state GeO, *J. Mol. Spectrosc.* 194 (1999) 197–202. doi:10.1006/jmsp.1998.7789.
- [45] J. M. Brown, A. J. Merer, Lambda-type doubling parameters for molecules in Π -electronic states of triplet and higher multiplicity, *J. Mol. Spectrosc.* 74 (1979) 488–494. doi:10.1016/0022-2852(79)90172-3.
- [46] Q. Qu, S. N. Yurchenko, J. Tennyson, Hyperfine-resolved variational nuclear motion spectra of diatomic molecules, *J. Chem. Theory Comput.* 18 (2022) 1808–1820. doi:10.1021/acs.jctc.1c01244.